HHS Public Access

Author manuscript

FASEB J. Author manuscript; available in PMC 2022 July 01.

Published in final edited form as:

FASEB J. 2021 July ; 35(7): e21719. doi:10.1096/fj.202100070R.

A novel role of ADGRF1 (GPR110) in promoting cellular quiescence and chemoresistance in human epidermal growth factor receptor 2-positive breast cancer

Noor Mazin Abdulkareem[1], **Raksha Bhat**[1,2], **Lanfang Qin**[3], **Suhas Vasaikar**[3], **Ambily Gopinathan**[2], **Tamika Mitchell**[3], **Martin J. Shea**[3], **Sarmistha Nanda**[3], **Hariprasad Thangavel**[2], **Bing Zhang**[3,4], **Carmine De Angelis**[3,5], **Rachel Schiff**[3,6,7], **Meghana V. Trivedi**[1,2,3,7]

[1]Department of Pharmacological and Pharmaceutical Sciences, University of Houston College of Pharmacy, Houston, TX, USA

[2]Department of Pharmacy Practice and Translational Research, University of Houston College of Pharmacy, Houston, TX, USA

[3]Lester and Sue Smith Breast Center, Baylor College of Medicine, Houston, TX, USA

[4]Department of Molecular and Human Genetics, Baylor College of Medicine, Houston, TX, USA

[5]Department of Clinical Medicine and Surgery, University of Naples, Federico II, Naples, Italy

[6]Department of Molecular and Cellular Biology, Baylor College of Medicine, Houston, TX, USA

[7]Department of Medicine, Baylor College of Medicine, Houston, TX, USA

Abstract

While G protein-coupled receptors (GPCRs) are known to be excellent drug targets, the second largest family of adhesion-GPCRs is less explored for their role in health and disease. ADGRF1 (GPR110) is an adhesion-GPCR and has an important function in neurodevelopment and cancer. Despite serving as a poor predictor of survival, ADGRF1's coupling to G proteins and downstream pathways remain unknown in cancer. We evaluated the effects of ADGRF1 overexpression on tumorigenesis and signaling pathways using two human epidermal growth factor receptor-2-positive (HER2+) breast cancer (BC) cell-line models. We also interrogated publicly available clinical datasets to determine the expression of ADGRF1 in various BC subtypes and its impact on BC-specific survival (BCSS) and overall survival (OS) in patients. ADGRF1 overexpression in HER2+ BC cells increased secondary mammosphere formation, soft

Correspondence: Meghana V. Trivedi, Department of Pharmacy Practice and Translational Research, University of Houston, Health 2, 4849 Calhoun Rd., Houston, TX 77204, USA. mtrivedi@central.uh.edu.
Noor Mazin Abdulkareem and Raksha Bhat are co-first authors.
Rachel Schiff and Meghana V. Trivedi are co-corresponding authors.

AUTHOR CONTRIBUTIONS

Noor Mazin Abdulkareem and Raksha Bhat performed the experiments and drafted the manuscript. Lanfang Qin, Tamika Mitchell, Martin J Shea, and Sarmistha Nanda performed and/or assisted with the experiments. Suhas Vasaikar, Carmine De Angelis, and Bing Zhang participated in bioinformatics analysis and data interpretation. Ambily Gopinathan, Hariprasad Thangavel, and Carmine De Angelis contributed with manuscript preparation and editing. Rachel Schiff and Meghana V. Trivedi conceived, designed and coordinated all the experiments and edited the manuscript. All authors read and approved the final manuscript.

SUPPORTING INFORMATION

Additional Supporting Information may be found online in the Supporting Information section.

agar colony formation, and % of Aldefluor-positive tumorigenic population in vitro and promoted tumor growth in vivo. ADGRF1 coimmunoprecipitated with both Gαs and Gαq proteins and increased cAMP and IP1 when overexpressed. However, inhibition of only the Gαs pathway by SQ22536 reversed the pro-tumorigenic effects of ADGRF1 overexpression. RNA-sequencing and RPPA analysis revealed inhibition of cell cycle pathways with ADGRF1 overexpression, suggesting cellular quiescence, as also evidenced by cell cycle arrest at the G0/1 phase and resistance to chemotherapy in HER2+ BC. *ADGRF1* was significantly overexpressed in the HER2-enriched BC compared to luminal A and B subtypes and predicted worse BCSS and OS in these patients. Therefore, ADGRF1 represents a novel drug target in HER2+ BC, warranting discovery of novel ADGRF1 antagonists.

Keywords

ADGRF1; breast cancer; chemoresistance; GPR110; HER2; quiescence; tumorigenesis

1 | INTRODUCTION

G protein-coupled receptors (GPCRs) are excellent drug targets due to their plasma membrane localization as well as high specificity and target-selectivity of ligands.[1] Over 30% of the Food and Drug Administration (FDA)-approved drugs target GPCRs and are used to treat a wide-range of chronic diseases, underscoring their overall favorable long-term safety profile.[2–4] While the pharmacology of the largest family of GPCRs (class A) is well defined with known biological functions for numerous receptors, very little is known about the second largest family of class B2 GPCRs, known as adhesion GPCRs.[5,6] Similar to other GPCRs, adhesion GPCRs couple to heterotrimeric G proteins to activate a variety of diverse downstream signaling pathways.[7] Adhesion GPCRs regulate cellular processes such as adhesion, polarity, invasion/migration, and stem cell function,[8–18] which are important in cancer. Thus, adhesion GPCRs may serve as important drug targets in cancer.[5]

ADGRF1 (previously known as GPR110) is a member of subfamily VI of adhesion GPCRs and is part of the druggable genome.[19] ADGRF1 is critical in neurodevelopment and neuro-inflammation.[20,21] Several studies have also suggested a role of ADGRF1 in tumorigenesis and metastasis pathways and in prediction of aggressive cancer. For example, overexpression of ADGRF1 is reported to induce more proliferation and/or invasion/migration in glioma[22] and osteosarcoma[23] cells. Higher ADGRF1 gene and protein expression is reported in patients with glioma[22] and in lung and prostate adenocarcinoma[24] compared to normal tissues and in tumor specimen with metastasis versus without metastasis in osteosarcoma patients.[23] In addition, ADGRF1 protein expression was higher in prostate cancer samples compared to benign prostatic hyperplasia[24] and correlated with the World Health Organization grading of glioma.[22] High ADGRF1 expression is also found in a unique cluster of pediatric patients with high-risk B-precursor acute lymphoblastic leukemia with very poor relapse-free survival.[25] Similarly, *ADGRF1* knockout mice showed reduced liver injury and fibrosis in response to carbon tetrachloride as well as resistance to carcinogen-induced hepatocellular carcinoma, suggesting the role of ADGRF1 in tumorigenesis.[26] Additionally, higher ADGRF1 expression is reported to be an independent predictor of poor

survival in patients with glioma,[22] osteosarcoma,[23] and gastric cancer.[27] Using knockdown approach, we previously identified ADGRF1 as a mediator of tumorigenesis in human epidermal growth factor receptor 2-positive (HER2+) breast cancer (BC).[28]

Despite an important role of ADGRF1 in cancer, its coupling to G proteins and downstream signaling pathways have not been evaluated in any type of cancer. In this study, our objectives were to (i) investigate the effects of ADGRF1 overexpression and evaluate its gain-of-function effects in HER2+ BC cells, (ii) identify the pharmacology and downstream molecular mechanisms behind ADGRF1 activity in HER2+ BC and (iii) evaluate *ADGRF1* genetic alterations and the clinical significance of *ADGRF1* overexpression in various BC subtypes by interrogating publicly available datasets. Our study confirms the role of ADGRF1 in promoting tumorigenesis in HER2+ BC. Our data illustrate that ADGRF1 couples to both Gαs and Gαq proteins, but its coupling to Gαs pathway is responsible for its pro-tumorigenic effects. We also reported a novel role of ADGRF1 in promoting cellular quiescence by inducing cell cycle arrest at the G0/1 phase, resulting in resistance to chemotherapy in HER2+ BC. Interrogation of clinical data show that *ADGRF1* is overexpressed in HER2-enriched BC subtype and predicts worse BC-specific and overall survival in these patients.

2 | MATERIALS AND METHODS

2.1 | Cell lines and reagents

The BT474 cell line was obtained from AstraZeneca (Cheshire, UK)[29] and maintained in Dulbecco's Modified Eagle Medium (DMEM) supplemented with 10% heat-inactivated fetal bovine serum (HI-FBS) and 1% penicillinstreptomycin-glutamine (PSG). SKBR3 cells were from Dr. Joe Gray's lab (Berkeley Lab, Berkeley, CA, USA) and were grown in McCoy's 5A with 10% HI-FBS and 1% PSG.[30,31] The gateway pLUS shuttle clone for ADGRF1 (catalog# GC-H0565-CF) was purchased from Genecopoeia, Rockville, MD, USA. The following antibodies were used in our studies: anti-HA (catalog# 26183, Thermo scientific), anti-phospho-EGF receptor/HER1 (Tyr845) (catalog# 2231S, Cell Signaling), anti-phospho-HER2/ErbB2 (Tyr1221/1222) (6B12) (catalog# 2243S, Cell Signaling), anti-EGF receptor/HER1 (E746-A750del Specific) (D6B6) (catalog# 2085S, Cell Signaling), anti-HER2/ErbB2 (29D8) (catalog# 2165S, Cell Signaling), anti-hADGRF1 (catalog# HPA038438, Atlas Antibodies), anti-Ki67 (clone MIB-1, Catalog# M7240, DAKO), anti-Gαs (catalog# 06–237-MI, Fisher Scientific), anti-Gαq (Catalog# 06–709-MI, Fisher Scientific), anti-GAPDH (catalog# ab9485, Abcam), anti-mouse horseradish peroxidase-conjugated secondary antibodies (catalog# 7076S, Cell Signaling), and anti-rabbit horseradish peroxidase-conjugated secondary antibodies (catalog# 7074S, Cell Signaling). The MTT kit (catalog# 30–1010K) was purchased from ATCC; the ALDEFLUOR kit (catalog# 01700) was from Stem Cell Technologies.

2.2 | Drugs

Doxycycline (Dox) hyclate (catalog# D9891) and G-418 (catalog# 4727878001) were purchased from Sigma Aldrich. Lapatinib [LC Laboratories (MA, USA)] and neratinib [Puma Biotechnology (CA, USA)] were dissolved in sterile dimethyl sulfoxide (DMSO).

[28,30] Drug dilutions were made in appropriate media such that the final DMSO concentration was less than 0.1%. Synaptamide (catalog# SML0563) was purchased from Sigma-Aldrich and was complexed with fatty acid-free bovine serum albumin in the presence of vitamin E as described previously.[21] Adenylyl cyclase (AC) activator (Forskolin) (catalog# 3442825MG) and inhibitor (SQ22536) (catalog# 5685005MG) and phospholipase C (PLC) activator (m-3M3FBS) (catalog# 52–518-510MG) and inhibitor (bisidolylmaleimide I hydrochloride (BIM I) (catalog# 20–329-01MG) were purchased from Fisher Scientific.

2.3 | Development of lentiviral plasmids containing ADGRF1 cDNA using the pHAGE system

Overexpression of ADGRF1 in parental BT474 and SKBR3 cells was obtained using Tet-On inducible lentiviral vector (pHAGE-ind-ubc-DEST) containing a c-terminal HA tag (a gift from Westbrook lab) as described before.[32] Selection of single cell colonies was conducted in presence of G-418 (1 mg/mL). A panel of single cell clones was tested for the expression of ADGRF1 upon Dox (2 μg/mL) treatment for 72 hours using anti-HA antibodies for immunoblotting and using TaqMan gene expression assay (Life-Technologies, USA) for quantitative polymerase chain reaction (qPCR).[28] Two clones, with high and medium expression, were selected for each cell line model for further analysis.

2.4 | Soft agar assay to assess anchorage-independent cell growth

Soft agar assay was performed as previously described.[28] Effect of lapatinib (1 nM) on anchorage-independent cell growth was also determined using the soft agar assay.

2.5 | Mammosphere assay

Mammocult Human medium kit (catalog# 05620) from Stem cell Technologies was used for the culturing of the mammospheres as previously described.[28] The secondary mammospheres were counted on Day 14 by Gelcount (Oxford Optronix, Germany).

2.6 | Aldefluor assay

The percentage of Aldefluor+ tumorigenic cell population was evaluated using ALDEFLUORTM kit. The analysis was performed using BD LSRFortessa cell analyzer as described before.[28]

2.7 | In vivo tumor growth

BT474 clone 1 cells were grown in the absence (−) or presence (+) of Dox for 72 hours. Xenografts were established by injecting 1 million cells subcutaneously into 5- to 6-week–old ovariectomized athymic (nu/nu) female mice (Envigo, Indianapolis, IN). Three days before cell injections, mice were supplemented with estrogen pellets as described before[33,34] and were randomized to be given drinking water with or without Dox (200 μg/mL). Cells grown without Dox were injected into mice receiving drinking water without Dox, and Dox-treated cells were injected into mice who received Dox for the entire experiment. Tumor diameters and body weight were assessed twice a week. The animal care for the mice was in accordance with the National Institutes of Health Guide for the Care and Use of

Experimental Animals with approval from the Baylor College of Medicine Institutional Animal Care and Use Committee.

2.8 | MTT assay

Cell growth and viability of the BT474 and SKBR3 clones containing ADGRF1 overexpressed in Dox-inducible manner was assessed using the MTT assay as previously described.[28] Various concentrations of docetaxel (10 pM – 10 μM), lapatinib (1 nM – 10 μM), and neratinib (10 pM – 10 μM) including vehicle were used in an 8-point concentration curve to determine the potency (IC_{50}) of the drug on cell growth.

2.9 | Co-immunoprecipitation

Membrane proteins were extracted from ADGRF1 overexpressing BT474 clone 1 and SKBR3 clone 2 cells grown in −Dox or +Dox for 72 hours Dox using a Mem-PER Plus Membrane Protein Extraction Kit (catalog# PI89842, Fisher Scientific). Immunoprecipitation was performed using a TrueBlot Anti-Rabbit Ig IP Agarose Bead (catalog# 00–8800-25, Rockland Immunochemical), as per manufacturer's protocol. Endogenous Gαs and Gαq were immunoprecipitated from membrane proteins (~500 μg of protein for each sample) using anti-Gαs and anti-Gαq. The samples were then subjected to SDS-PAGE and immunoblotted using anti-HA, anti-Gαs and anti-Gαq antibodies.

2.10 | Immunoblotting

The immunoblotting to detect expression of various proteins was performed as described before.[35]

2.11 | cAMP and IP1 assays

Cyclic adenosine monophosphate (cAMP) levels were assessed using AlphaScreen cAMP detection kit, (catalog# 6760635, PerkinElmer). Inositol monophosphate (IP1) levels were assessed using the IP-One kit, (catalog# 62IPAPEB, Cisbio). Both AlphaScreen and Homogeneous Time Resolved Fluorescence (HTRF) signals were assessed on EnSight multimode plate reader.

2.12 | RNA-Sequencing (RNAseq) and analysis of data

BT474 clones 1 and 5 were grown in −Dox or +Dox for 72 hours. Total RNA extraction was done using a miRNE-asy micro kit from Qiagen (catalog# 217084) following manufacturer's instructions. RNA samples underwent quality control assessment using the RNA tape on Tapestation 4200 (Agilent) and were quantified with Qubit Fluorometer (Thermo Fisher). The RNA libraries were prepared and sequenced at the University of Houston Sequencing and Gene Editing core per standard protocols. RNA libraries were prepared with QIAseq Stranded Total RNA library Kit (Qiagen) using 500 ng input RNA. mRNA was enriched with Oligo-dT probes attached to Pure mRNA beads (Qiagen). RNA was fragmented, reverse transcribed into cDNA, and ligated with Illumina sequencing adaptors. The size selection for libraries was performed using SPRIselect beads (Beckman Coulter) and purity of the libraries was analyzed using the DNA 1000 tape Tapestation 4200 (Agilent). The indexed libraries were pooled and sequenced using NextSeq 500 (Illumina);

generating ~20 million 2 × 76 bp paired-end reads per samples. We used RNAseq data to identify potential biological processes that were associated with ADGRF1 activity. The common differentially expressed upregulated and downregulated genes for BT474 clones 1 and 5 were used to perform the over-representation analysis (ORA)-based enrichment analysis[36] using Kyoto Encyclopedia of Genes and Genomes (KEGG) database.[37]

2.13 | Reverse-phase protein array and analysis of data

BT474 (clones 1 and 5) and SKBR3 (clones 1 and 2) were grown in −Dox or +Dox conditions for 72 hours. Reverse-phase protein array (RPPA) analysis was performed as described previously.[38,39] A false discovery rate (FDR) adjusted p-value (*q*-value) threshold of 0.05 was used to define differentially expressed proteins between +Dox vs −Dox cells.

2.14 | Cell cycle analysis

ADGRF1 overexpressing BT474 clone 1 and clone 5 were grown in −Dox or +Dox in a six-well plate (1×10^6 cells/well) for 72 hours. Then, cells were trypsinized and fixed with 70% ethanol and kept at −20°C overnight. After the fixation, the cell pellet was resuspended in RNase A (100 μg/ml) and 0.1% Triton X-100 and propidium iodide and incubated for 30 minutes at 37°C. Cell cycle distribution was analyzed by LSRFortessa cell analyzer.

2.15 | Immunohistochemistry

Pellets from ADGRF1-overexpressing BT474 clones 1 and 5 cells grown in −Dox or +Dox for 72 hours or tumors harvested from mice were fixed in 10% neutral buffered formalin and paraffin embedded. Immunohistochemistry (IHC) was conducted as previously described.[39,40]

2.16 | Bioinformatics analysis of public datasets

The normalized values of *ADGRF1* mRNA expression and copy number in panel of HER2+ cell lines were downloaded from the publicly available Cancer Cell Line Encyclopedia (CCLE) dataset[41] and plotted using GraphPad Prism version 8.1c. The Firehose GDAC portal was used to download processed The Cancer Genome Atlas (TCGA) RNA-Seq (Illumina HiSeq) and SNP6 copy number (GISTIC2) data (http://gdac.broadinstitute.org/). The log2 transformed normalized RSEM (RNA-Seq by Expectation Maximization) count data for tumor samples (n = 1093) were extracted. The PAM50 annotation was used for BC samples with Luminal A (n = 415), Luminal B (n = 176), Basal (n = 136) and HER2-enriched (n = 65) as previously described.[42] The statistical analysis was performed using the computing environment R (3.5.2). Survival analyses were performed using Molecular Taxonomy of Breast Cancer International Consortium (METABRIC) dataset comprising of 2433 primary breast tumors.[43] The impact of *ADGRF1* gene expression on BC-specific survival (BCSS) and overall survival (OS) was determined in patients with HER2-enriched (n = 220) and basal subtypes (n = 199) by PAM50. For survival analysis, cox proportional model was applied on continuous gene expression and the plots were generated with high *ADGRF1* group (>median) and low *ADGRF1* expression (≤median).[44]

2.17 | Statistical analyses

All cell-based studies were conducted at least three independent times, each in triplicates. All data analysis was done using the GraphPad Prism version 8.1c. Values were presented as mean ± SEM unless otherwise specified. Statistical differences between the groups were analyzed by student's *t* test or two-way analysis of variance (ANOVA) followed by Dunnett's multiple comparison post hoc test, as appropriate. A *P*-value of < .05 was considered statistically significant. Kaplan-Meier survival curves were generated to show differences in BCSS and OS. The *P*-values were generated using log-rank (Mantel-Cox) test to determine differences in survival in patients with high versus low *ADGRF1* mRNA expression on tumors in various subtypes of BC.

3 | RESULTS

3.1 | Generation of stable ADGRF1 overexpressing clones

In the publicly available CCLE dataset,[41] BT474 (hormone receptor-positive (HR+)) and SKBR3 (HR−) cell line models of HER2+ BC had low *ADGRF1* mRNA and copy number values, and hence were chosen to generate the stable ADGRF1 overexpressing clones (Figure 1A). Two stable clones of each BT474 and SKBR3 cells containing pHAGE lentiviral plasmid system with ADGRF1 cDNA were selected based on high and moderate ADGRF1 overexpression upon Dox treatment (Figure 1B). ADGRF1 overexpression in BT474 clones 1 and 5 and SKBR3 clones 1 and 2 was confirmed in +Dox versus −Dox conditions using anti-HA (Figure 1B) and anti-human ADGRF1 (Figure S1) antibodies by immunoblotting and using TaqMan probes for qPCR (Figure 1C,D). Dox-induced ADGRF1 overexpression in the clones was confirmed using immunoblotting and/or qPCR every 1–2 months during all studies.

3.2 | ADGRF1 overexpression promotes tumorigenesis in HER2+ BC in vitro and in vivo

Dox-induced ADGRF1 overexpression resulted in a significant increase in the number of colonies in the soft agar assay in both BT474 (Figure 2A) and SKBR3 (Figure 2B) cell line clones. Likewise, ADGRF1 overexpression resulted in enhanced secondary mammosphere formation (Figure 2C), and a higher Aldefluor+ tumorigenic population of BT474 clones (42% vs 19% in clone 1 and 50% vs 27% in clone 5) (Figure 2D). Doxycycline by itself had no effects on mammosphere formation in parental BT474 cells (Figure S2). The SKBR3 cells did not form mammospheres, and hence were not evaluated for the effect of ADGRF1 overexpression. In mice, tumor growth rate was faster with ADGRF1 overexpression, which was confirmed by IHC using anti-HA antibodies in the harvested tumors (Figure 2E).

3.3 | ADGRF1 overexpression has no effects on HER pathways in HER2+ BC

There was no significant change observed in the expression levels of phosphorylated- and total-HER1 and HER2 protein levels upon ADGRF1 overexpression in any of the BT474 and SKBR3 clones (Figure 3A,B). ADGRF1 overexpression also did not alter the potency (IC_{50}) or efficacy of (Emax) of lapatinib (an anti-HER2 drug) on cell growth inhibition in BT474 and SKBR3 clones (Figure 4A,B). We confirmed the same results using a more potent anti-HER2 agent, neratinib, in −Dox vs +Dox-treated BT474 clones (Figure S3). The

calculated lapatinib and neratinib IC_{50} values are reported in (Table 1). In addition, lapatinib 1 nM inhibited colony formation to a similar extent in both −Dox and +Dox-treated clones of BT474 (Figure 4C,D) and SKBR3 cells (Figure 4E,F).

3.4 | ADGRF1 couples to and activates Gαs and Gαq pathways in HER2+ BC

ADGRF1 coimmunoprecipitated with Gαs subunit in both BT474 clone 1 and SKBR3 clone 2 cells upon ADGRF1 overexpression with Dox (Figure 5A). In addition, basal level of cAMP, an indicator of Gαs activation, was significantly higher in +Dox vs −Dox treated cells (Figure 5B). Similarly, ADGRF1 also coimmunoprecipitated with Gαq subunit in BT474 clone 1 and SKBR3 clone 2 cells treated with Dox (Figure 5C). The basal level of IP1, an indicator of Gαq activation, was significantly higher in +Dox versus −Dox treated BT474 clone 1 but not SKBR3 clone 2 cells (Figure 5D).

3.5 | ADGRF1 coupling to Gαs pathway is pro-tumorigenic

SQ22536 (Gαs pathway inhibitor) significantly reduced the number of secondary mammospheres only in cells with ADGRF1 overexpression with +Dox but not −Dox (Figure 6A). Whereas, Forskolin (Gαs pathway activator) significantly increased mammosphere formation with or without ADGRF1 overexpression (Figure 6B). These findings suggest a pro-tumorigenic effect of ADGRF1 coupling to the Gαs pathway. On the other hand, BIM I (Gαq pathway inhibitor) significantly increased (Figure 6A) and m-3M3FBS (Gαq pathway activator) significantly decreased (Figure 6B) the number of secondary mammospheres compared to vehicle in cells with and without ADGRF1 overexpression. These findings indicate that ADGRF1 coupling to Gαq pathway may not impact tumorigenesis. ADGRF1 agonist, synaptamide, did not have any effects on secondary mammosphere formation potential in ADGRF1 overexpressing BT474 clone 1 (Figure 6B). Synaptamide also did not affect the basal levels of cAMP (Figure 6C,D) and IP1 (Figure 6E,F) in ADGRF1 overexpressing BT474 clone 1 and SKBR3 clone 2 cells. While only 10 nM synaptamide data is shown here, we also did not find any significant difference in cAMP or IP1 levels with multiple synaptamide concentrations (0.1, 1, 10, 100, and 1000 nM) in parental BT474, −Dox, and +Dox (0.02 and 2 μg/ml) cells (Figures S4 and S5). Lower concentration of Dox was used to moderately overexpress ADGRF1. Likewise, synaptamide (1, 10, and 100 nM) did not increase cAMP in BT474 clone 5 and SKBR3 clone 1 cells (Figure S6) with moderate Dox-induced ADGRF1 overexpression as shown in Figure 1B.

3.6 | ADGRF1 overexpression induced cell cycle arrest and chemoresistance indicating a state of quiescence in HER2+ BC

In the ORA-based enrichment analysis of the RNAseq data of ADGRF1 overexpression, we identified two significantly downregulated pathways (FDR < 0.05) of cell cycle and oocyte meiosis (Figure 7A). None of the upregulated pathways were enriched significantly. The differentially expressed proteins from RPPA analysis also revealed a downregulation of multiple proteins involved in the cell cycle (FDR < 0.05) upon ADGRF1 overexpression in BT474 clones 1 and 5 cells (Figure 7B). The complete lists of individually and commonly up- and down-regulated proteins with FDR < 0.05 upon ADGRF1 overexpression in BT474 clones 1 and 5 and in SKBR3 clones 1 and 2 are shown in Figure S7. Cell cycle analysis indicated a G0/1 arrest (% of cells in −Dox vs +Dox: 68 versus 87 and 70 versus 91 in

BT474 clone 1 and 5, respectively) (Figure 7C). We also confirmed the reduction in the expression of Ki67, a proliferation marker, upon ADGRF1 overexpression by IHC in BT474 (% Ki76-positive cells in −Dox versus +Dox: 87 versus 15 and 91 versus 19 in BT474 clone 1 and 5, respectively) (Figure 7D) and SKBR3 models (% Ki76-positive cells in −Dox versus +Dox: 73 versus 21 and 79 versus 15 in SKBR3 clone 1 and 2, respectively) (Figure S7D). The potency (IC_{50}) of docetaxel (Table 2), a chemotherapy drug clinically used in HER2+ BC, was reduced by 10-fold upon ADGRF1 overexpression (Figure 7E).

3.7 | *ADGRF1* is overexpressed/amplified in HER2-enriched subtype and predicts poor BCSS and OS in patients

Interrogation of TCGA BC patient data revealed that in primary breast tumors, *ADGRF1* gene expression was significantly higher in HER2-enriched and basal subtypes compared to luminal A and B BCs (Figure 8A). In addition, *ADGRF1* gene was amplified in HER2-enriched and basal BC, with basal subtype having the highest gene amplification (Figure 8B). Using the METABRIC dataset, we found that HER2-enriched BC patients with high *ADGRF1* mRNA expression had worse BCSS ($P = 0.023$, Figure 8C) and OS ($P = 0.0275$, Figure 8D) compared to those with low *ADGRF1* mRNA expression. However, BCSS and OS were not significantly altered by higher *ADGRF1* expression in basal-like BC patients (BCSS, $P = 0.82$, Figure 8E and OS, $P = 0.768$, Figure 8F). We also found that BCSS and OS were not significantly different with higher expression of *GNAS or GNAQ,* coding for Gαs and Gαq, respectively, in both HER2-enriched and basal-like BC patients (Figure S8). In addition, the frequency of mutation in *GNAS* was very low (0.6%), and *GNAQ* mutations were not detected in HER2+ BC as shown in Figure S9.

4 | DISCUSSION

In the present study, we report that overexpression of the adhesion GPCR, ADGRF1, significantly increased the colony formation, secondary mammosphere formation, and Aldefluor+ cells in vitro and promoted tumor growth in vivo. However, ADGRF1 overexpression had no effect on phosphorylated- and total-HER1 and HER2 expression or on the potency or sensitivity of anti-HER2 drugs in HER2+ BC. We found that ADGRF1 coupled to both Gαs and Gαq pathways in HER2+ BC cells. Reduction of ADGRF1-driven mammosphere formation by a Gαs pathway inhibitor only in ADGRF1-overexpressing cells suggested pro-tumorigenic effects of the ADGRF1 coupling to the Gαs protein. ADGRF1 overexpression also led to cell cycle arrest and resistance to docetaxel, indicating a state of cellular quiescence in HER2+ BC cells. *ADGRF1* was overexpressed and amplified in HER2-enriched tumors and was a poor prognostic factor for BCSS and OS in patients.

The gain of function finding in our study with ADGRF1 overexpression is in agreement with our previous study where ADGRF1 knockdown caused significant inhibition in colony formation and mammosphere formation.[28] Our data concur with other studies showing a role of ADGRF1 in promoting oncogenesis and the role of ADGRF1 as a poor prognostic factor in predicting outcomes in patients with various cancer types.[22–24,27,45] The findings of no effect of ADGRF1 overexpression on HER1/HER2 expression or phosphorylation and on activity of anti-HER2 drugs are consistent with our previous study using *ADGRF1*

knockdown.[28] However, the role of ADGRF1 in the development of anti-HER2 drug resistance and its reversal remains unknown and needs further investigation.

While the pharmacology of ADGRF1 has been investigated, its activation mechanisms and G protein coupling remain a topic of debate. There are two proposed mechanisms of ADGRF1 activation: (i) by synaptamide, an endogenous ligand, and (ii) by the cryptic tethered peptide agonist exposed after the dissociation of the N-terminus fragment (NTF). One group has reported that ADGRF1 is activated by synaptamide and couples to only Gαs protein leading to AC-cAMP-protein kinase A (PKA) activation and promoting neurogenesis.[21] However, they showed that the NTF dissociation was unnecessary to activate ADGRF1.[46] Another group has reported that ADGRF1 is activated by the exposed cryptic tethered peptide agonist after the NTF dissociation and couples to Gαq and not Gαs proteins.[47] This group also reported that synaptamide did not activate ADGRF1 in their biochemical reconstitution assays,[48] whereas a third group reported that endogenous ADGRF1 in renal papilla could couple to Gαs upon activation by the agonistic peptide.[49] Our results suggest that ADGRF1 couples to both Gαs and Gαq in HER2+ BC cells. While we identified ADGRF1 co-IP'ed with Gαq, we were not able to detect an increase in the IP1 level in ADGRF1-overexpressing SKBR3 cells, which may be due to low assay sensitivity. While we detected a lower molecular weight band (~25 kDa) in +Dox cells, it is not clear whether this is the cleaved C-terminus fragment of ADGRF1 after NTF dissociation. The reason behind the lack of synaptamide effects in our studies is not clear. We speculate that a very high basal level of cAMP and IP1 in the +Dox cells (BT474 and SKBR3) and a very low ADGRF1 expression in parental and −Dox cells (SKBR3 cells) may result in the absence of synaptamide activity. It is also possible that synaptamide acts in a cell-specific manner, which may explain its lack of effects in HER2+ BC cells. In contrast, we have found that synaptamide increases cAMP, not IP1, in a triple-negative BC cell line, which is reported to have ADGRF1 gene amplification and overexpression (data not shown). The differential effects of synaptamide in various BC cell lines are currently under investigation.

The downstream signaling pathways associated with ADGRF1 activity in cancer are largely unknown. Our study suggests that coupling of ADGRF1 to Gαs pathway is responsible for its pro-tumorigenic effects. Consistent with these findings, cAMP-dependent PKA, is known to play a role in the onset and progression of various tumors.[50–54] Also, PKA has been reported to have a crucial role in driving mammary tumorigenesis[50] and inducing cell cycle arrest.[55,56] These reports are consistent with our findings of cell cycle arrest at G0/1 and reduction in Ki67 expression upon ADGRF1 overexpression. Interestingly, ADGRF1 overexpression also reduces sensitivity to chemotherapy drug, docetaxel, suggesting chemoresistance. The inhibition of cell cycle is a critical mechanism by which tumorigenic cells remain reversibly quiescent and are resistant to chemotherapy.[57–60] To the best of our knowledge, our present study is the first suggesting a role of an adhesion GPCR in regulating cell cycle, inducing cellular quiescence, and chemoresistance. Several *GNAS* or *GNAQ* mutations are reported to affect tumorigenesis in various cancer types.[61] However, low frequency of these mutations and the lack of predictive role of higher *GNAS* or *GNAQ* expression on BCSS and OS in HER2+ BC also rules out their effects on the predictive role of ADGRF1 on survival in HER2+ BC patients.

In conclusion, ADGRF1 overexpression results in pro-tumorigenic behavior of HER2+ BC in vitro and in vivo and is associated with worse outcomes in HER2-enriched BC patients. The pro-tumorigenic feature of ADGRF1 is mediated via its coupling to the Gαs pathway. ADGRF1 overexpression induces cellular quiescence in HER2+ BC cells, which is a reversible feature of tumorigenic cells, and confers chemoresistance. Therefore, ADGRF1 represents a novel drug target, warranting discovery of novel ADGRF1 antagonists.

Supplementary Material

Refer to Web version on PubMed Central for supplementary material.

ACKNOWLEDGMENTS

This work was supported in parts by Department of Defense BCRP grants W81XWH-14-1-0340 and W81XWH-14-1-0341; Breast Cancer Research Foundation (BCRF-18-145 and 19-145 grants); and NIH grants CA125123, P50 CA058183, and CA186784-01. None of the funding agencies had any role in the design, analysis, or reporting of the analyses. The authors thank Joe Gray and Thomas Westbrook labs for providing SKBR3 cells and lentiviral vector (pHAGE-ind-ubc-DEST) containing a c-terminal HA tag, respectively. We also thank Dr. Shixia Huang from the Antibody-based Proteomics Core/Shared Resource and Dr. Preethi Gunaratne, Dr. Kimberly Holloway, and Mr. Brandon Mistretta from the UH Seq-N-Edit Core for their excellent technical assistant in performing RPPA and RNA-Seq studies, respectively.

CONFLICT OF INTEREST

Rachel Schiffhas received research support from AstraZeneca, GlaxoSmithKline, Gilead, and Puma Biotechnology. Rachel Schiff served as an ad hoc consultant to Eli Lilly and is a paid consultant/advisory board member for MacroGenics. Carmine De Angelis has served as consultant/advisory board member for Eli Lilly, GSK, Novartis, Pfizer. Carmine De Angelis has received research support from Novartis. All other authors declare no conflict of interest.

Abbreviations:

AC	adenylyl cyclase
ANOVA	analysis of variance
BC	breast cancer
BCSS	breast cancer-specific survival
BIM I	bisindolylmaleimide I
cAMP	cyclic adenosine monophosphate
CCLE	cancer cell line encyclopedia
Dox	doxycycline
FDR	false discovery rate
GPCRs	G protein-coupled receptors
HER	human epidermal growth factor receptor
HER2+	human epidermal growth factor receptor 2-positive

HR	hormone receptor
HTRF	homogeneous time-resolved fluorescence
IHC	immunohistochemistry
IP1	inositol monophosphate
METABRIC	molecular taxonomy of breast cancer international consortium
NTF	N-terminus fragment
ORA	over-representation analysis
OS	overall survival
PKA	protein kinase A
PKC	protein kinase C
PLC	phospholipase C
qPCR	quantitative polymerase chain reaction
RNAseq	RNA sequencing
RPPA	reverse phase protein arrays
TCGA	the cancer genome atlas

REFERENCES

1. Hauser AS, Attwood MM, Rask-Andersen M, Schioth HB, Gloriam DE. Trends in GPCR drug discovery: new agents, targets and indications. Nat Rev Drug Discov. 2017;16(12):829–842. 10.1038/nrd.2017.178 [PubMed: 29075003]
2. Santos R, Ursu O, Gaulton A, et al. A comprehensive map of molecular drug targets. Nat Rev Drug Discov. 2017;16(1):19–34. 10.1038/nrd.2016.230 [PubMed: 27910877]
3. Rask-Andersen M, Almen MS, Schioth HB. Trends in the exploitation of novel drug targets. Nat Rev Drug Discov. 2011;10(8):579–590. 10.1038/nrd3478 [PubMed: 21804595]
4. Dorsam RT, Gutkind JS. G-protein-coupled receptors and cancer. Nat Rev Cancer. 2007;7(2):79–94. 10.1038/nrc2069 [PubMed: 17251915]
5. Vizurraga A, Adhikari R, Yeung J, Yu M, Tall GG. Mechanisms of adhesion G protein-coupled receptor activation. J Biol Chem. 2020;295(41): 14065–14083. 10.1074/jbc.REV120.007423 [PubMed: 32763969]
6. Schioth HB, Fredriksson R. The GRAFS classification system of G-protein coupled receptors in comparative perspective. Gen Comp Endocrinol. 2005;142(1–2):94–101. 10.1016/j.ygcen.2004.12.018 [PubMed: 15862553]
7. Gad AA, Balenga N. The emerging role of adhesion GPCRs in cancer. ACS Pharmacol Transl Sci. 2020;3(1):29–42. 10.1021/acsptsci.9b00093 [PubMed: 32259086]
8. Ward Y, Lake R, Faraji F, et al. Platelets promote metastasis via binding tumor CD97 leading to bidirectional signaling that coordinates transendothelial migration. Cell Rep. 2018;23(3):808–822. 10.1016/j.celrep.2018.03.092 [PubMed: 29669286]
9. Moreno M, Pedrosa L, Paré L, et al. GPR56/ADGRG1 inhibits mesenchymal differentiation and radioresistance in glioblastoma. Cell Rep. 2017;21(8):2183–2197. 10.1016/j.celrep.2017.10.083 [PubMed: 29166609]

10. Aust G, Zhu D, Van Meir EG, Xu L. Adhesion GPCRs in tumorigenesis. Handb Exp Pharmacol. 2016;234:369–396. 10.1007/978-3-319-41523-9_17 [PubMed: 27832497]
11. Knapp B, Wolfrum U. Adhesion GPCR-related protein networks. Handb Exp Pharmacol. 2016;234:147–178. 10.1007/978-3-319-41523-9_8 [PubMed: 27832488]
12. Kishore A, Hall RA. Versatile signaling activity of adhesion GPCRs. Handb Exp Pharmacol. 2016;234:127–146. 10.1007/978-3-319-41523-9_7 [PubMed: 27832487]
13. Peeters MC, Fokkelman M, Boogaard B, et al. The adhesion G protein-coupled receptor G2 (ADGRG2/GPR64) constitutively activates SRE and NFkappaB and is involved in cell adhesion and migration. Cell Signal. 2015;27(12):2579–2588. 10.1016/j.cellsig.2015.08.015 [PubMed: 26321231]
14. Valtcheva N, Primorac A, Jurisic G, Hollmen M, Detmar M. The orphan adhesion G protein-coupled receptor GPR97 regulates migration of lymphatic endothelial cells via the small GTPases RhoA and Cdc42. J Biol Chem. 2013;288(50):35736–35748. 10.1074/jbc.M113.512954 [PubMed: 24178298]
15. Tang X, Jin R, Qu G, et al. GPR116, an adhesion G-protein-coupled receptor, promotes breast cancer metastasis via the Galphaq-p63RhoGEF-Rho GTPase pathway. Cancer Res. 2013;73(20):6206–6218. 10.1158/0008-5472.CAN-13-1049 [PubMed: 24008316]
16. Langenhan T, Aust G, Hamann J. Sticky signaling-adhesion class G protein-coupled receptors take the stage. Sci Signal. 2013;6(276):re3. 10.1126/scisignal.2003825. [PubMed: 23695165]
17. Langenhan T, Promel S, Mestek L, et al. Latrophilin signaling links anterior-posterior tissue polarity and oriented cell divisions in the *C. elegans* embryo. Dev Cell. 2009;17(4):494–504. 10.1016/j.devcel.2009.08.008 [PubMed: 19853563]
18. Yona S, Lin H-H, Dri P, et al. Ligation of the adhesion-GPCR EMR2 regulates human neutrophil function. FASEB J. 2008;22(3):741–751. 10.1096/fj.07-9435com [PubMed: 17928360]
19. Scholz N, Langenhan T, Schoneberg T. Revisiting the classification of adhesion GPCRs. Ann N Y Acad Sci. 2019;1456(1):80–95. 10.1111/nyas.14192 [PubMed: 31365134]
20. Park T, Chen H, Kim HY. GPR110 (ADGRF1) mediates anti-inflammatory effects of N-docosahexaenoylethanolamine. J Neuroinflammation. 2019;16(1):225. 10.1186/s12974-019-1621-2 [PubMed: 31730008]
21. Lee J-W, Huang BX, Kwon H, et al. Orphan GPR110 (ADGRF1) targeted by N-docosahexaenoylethanolamine in development of neurons and cognitive function. Nat Commun. 2016;7:13123. 10.1038/ncomms13123 [PubMed: 27759003]
22. Shi H, Zhang S. Expression and prognostic role of orphan receptor GPR110 in glioma. Biochem Biophys Res Commun. 2017;491(2):349–354. 10.1016/j.bbrc.2017.07.097 [PubMed: 28728843]
23. Liu Z, Zhang G, Zhao C, Li J. Clinical significance of G protein-coupled receptor 110 (GPR110) as a novel prognostic biomarker in osteosarcoma. Med Sci Monit. 2018;24:5216–5224. 10.12659/MSM.909555 [PubMed: 30052620]
24. Lum AM, Wang BB, Beck-Engeser GB, Li L, Channa N, Wabl M. Orphan receptor GPR110, an oncogene overexpressed in lung and prostate cancer. BMC Cancer. 2010;10:40. 10.1186/1471-2407-10-40 [PubMed: 20149256]
25. Harvey RC, Mullighan CG, Wang X, et al. Identification of novel cluster groups in pediatric high-risk B-precursor acute lymphoblastic leukemia with gene expression profiling: correlation with genome-wide DNA copy number alterations, clinical characteristics, and outcome. Blood. 2010;116(23):4874–4884. 10.1182/blood-2009-08-239681 [PubMed: 20699438]
26. Ma B, Zhu J, Tan J, et al. Gpr110 deficiency decelerates carcinogen-induced hepatocarcinogenesis via activation of the IL-6/STAT3 pathway. Am J Cancer Res. 2017;7(3):433–447. [PubMed: 28401002]
27. Zhu X, Huang G, Jin P. Clinicopathological and prognostic significance of aberrant G protein-couple receptor 110 (GPR110) expression in gastric cancer. Pathol Res Pract. 2019;215(3):539–545. 10.1016/j.prp.2018.12.004 [PubMed: 30638950]
28. Bhat RR, Yadav P, Sahay D, et al. GPCRs profiling and identification of GPR110 as a potential new target in HER2+ breast cancer. Breast Cancer Res Treat. 2018;170(2):279–292. 10.1007/s10549-018-4751-9 [PubMed: 29574636]

29. Arpino G, Gutierrez C, Weiss H, et al. Treatment of human epidermal growth factor receptor 2-overexpressing breast cancer xenografts with multiagent HER-targeted therapy. J Natl Cancer Inst. 2007;99(9):694–705. 10.1093/jnci/djk151 [PubMed: 17470737]
30. Wang Y-C, Morrison G, Gillihan R, et al. Different mechanisms for resistance to trastuzumab versus lapatinib in HER2-positive breast cancers-role of estrogen receptor and HER2 reactivation. Breast Cancer Res. 2011;13(6):R121. 10.1186/bcr3067 [PubMed: 22123186]
31. Huang C, Park CC, Hilsenbeck SG, et al. Beta1 integrin mediates an alternative survival pathway in breast cancer cells resistant to lapatinib. Breast Cancer Res. 2011;13(4):R84. 10.1186/bcr2936 [PubMed: 21884573]
32. Meerbrey KL, Hu G, Kessler JD, et al. The pINDUCER lentiviral toolkit for inducible RNA interference in vitro and in vivo. Proc Natl Acad Sci U S A. 2011;108(9):3665–3670. 10.1073/pnas.1019736108 [PubMed: 21307310]
33. Nardone A, Weir H, Delpuech O, et al. The oral selective oestrogen receptor degrader (SERD) AZD9496 is comparable to fulvestrant in antagonising ER and circumventing endocrine resistance. Br J Cancer. 2019;120(3):331–339. 10.1038/s41416-018-0354-9 [PubMed: 30555156]
34. Ariazi EA, Lewis-Wambi JS, Gill SD, et al. Emerging principles for the development of resistance to antihormonal therapy: implications for the clinical utility of fulvestrant. J Steroid Biochem Mol Biol. 2006;102(1–5):128–138. 10.1016/j.jsbmb.2006.09.003 [PubMed: 17085047]
35. Sethunath V, Hu H, De Angelis C, et al. Targeting the mevalonate pathway to overcome acquired anti-HER2 treatment resistance in breast cancer. Mol Cancer Res. 2019;17(11):2318–2330. 10.1158/1541-7786.MCR-19-0756 [PubMed: 31420371]
36. Liao Y, Wang J, Jaehnig EJ, Shi Z, Zhang B. WebGestalt 2019: gene set analysis toolkit with revamped UIs and APIs. Nucleic Acids Res. 2019;47(W1):W199–W205. 10.1093/nar/gkz401 [PubMed: 31114916]
37. Kanehisa M, Goto S. KEGG: kyoto encyclopedia of genes and genomes. Nucleic Acids Res. 2000;28(1):27–30. 10.1093/nar/28.1.27 [PubMed: 10592173]
38. Thangavel H, Angelis CD, Vasaikar S, et al. A CTC-cluster-specific signature derived from OMICS analysis of patient-derived xenograft tumors predicts outcomes in basal-like breast cancer. J Clin Med. 2019;8(11):1772. 10.3390/jcm8111772
39. Zhang X, Claerhout S, Prat A, et al. A renewable tissue resource of phenotypically stable, biologically and ethnically diverse, patient-derived human breast cancer xenograft models. Cancer Res. 2013;73(15):4885–4897. 10.1158/0008-5472.CAN-12-4081 [PubMed: 23737486]
40. Nair A, Chung H-C, Sun T, et al. Combinatorial inhibition of PTPN12-regulated receptors leads to a broadly effective therapeutic strategy in triple-negative breast cancer. Nat Med. 2018;24(4):505–511. 10.1038/nm.4507 [PubMed: 29578538]
41. Barretina J, Caponigro G, Stransky N, et al. The cancer cell line encyclopedia enables predictive modelling of anticancer drug sensitivity. Nature. 2012;483(7391):603–607. 10.1038/nature11003 [PubMed: 22460905]
42. Ciriello G, Gatza M, Beck A, et al. Comprehensive molecular portraits of invasive lobular breast cancer. Cell. 2015;163(2):506–519. 10.1016/j.ell.2015.09.033 [PubMed: 26451490]
43. Pereira B, Chin SF, Rueda OM, et al. The somatic mutation profiles of 2,433 breast cancers refines their genomic and transcriptomic landscapes. Nat Commun. 2016;7:11479. 10.1038/ncomms11479 [PubMed: 27161491]
44. Vasaikar SV, Straub P, Wang J, Zhang B. LinkedOmics: analyzing multi-omics data within and across 32 cancer types. Nucleic Acids Res. 2018;46(D1):D956–D963. 10.1093/nar/gkx1090 [PubMed: 29136207]
45. Hasan AN, Ahmad MW, Madar IH, Grace BL, Hasan TN. An in silico analytical study of lung cancer and smokers datasets from gene expression omnibus (GEO) for prediction of differentially expressed genes. Bioinformation. 2015;11(5):229–235. 10.6026/97320630011229 [PubMed: 26124566]
46. Huang BX, Hu X, Kwon H-S, et al. Synaptamide activates the adhesion GPCR GPR110 (ADGRF1) through GAIN domain binding. Commun Biol. 2020;3(1):109. 10.1038/s42003-020-0831-6 [PubMed: 32144388]

47. Stoveken HM, Hajduczok AG, Xu L, Tall GG. Adhesion G protein-coupled receptors are activated by exposure of a cryptic tethered agonist. Proc Natl Acad Sci USA. 2015;112(19):6194–6199. 10.1073/pnas.1421785112 [PubMed: 25918380]

48. Stoveken HM, Larsen SD, Smrcka AV, Tall GG. Gedunin- and Khivorin-derivatives are small-molecule partial agonists for adhesion G protein-coupled receptors GPR56/ADGRG1 and GPR114/ADGRG5. Mol Pharmacol. 2018;93(5):477–488. 10.1124/mol.117.111476 [PubMed: 29476042]

49. Demberg LM, Winkler J, Wilde C, et al. Activation of adhesion G protein-coupled receptors: agonist specificity of stachel sequence-derived peptides. J Biol Chem. 2017;292(11):4383–4394. 10.1074/jbc.M116.763656 [PubMed: 28154189]

50. Beristain AG, Molyneux SD, Joshi PA, et al. PKA signaling drives mammary tumorigenesis through Src. Oncogene. 2015;34(9):1160–1173. 10.1038/onc.2014.41 [PubMed: 24662820]

51. McKenzie AJ, Campbell SL, Howe AK. Protein kinase A activity and anchoring are required for ovarian cancer cell migration and invasion. PLoS One. 2011;6(10):e26552. 10.1371/journal.pone.0026552e26552 [PubMed: 22028904]

52. Caretta A, Mucignat-Caretta C. Protein kinase a in cancer. Cancers (Basel). 2011;3(1):913–926. 10.3390/cancers3010913 [PubMed: 24212646]

53. Almeida MQ, Stratakis CA. How does cAMP/protein kinase A signaling lead to tumors in the adrenal cortex and other tissues? Mol Cell Endocrinol. 2011;336(1–2):162–168. 10.1016/j.mce.2010.11.018 [PubMed: 21111774]

54. Jiang P, Enomoto A, Takahashi M. Cell biology of the movement of breast cancer cells: intracellular signalling and the actin cytoskeleton. Cancer Lett. 2009;284(2):122–130. 10.1016/j.canlet.2009.02.034 [PubMed: 19303207]

55. Zambon AC, Zhang L, Minovitsky S, et al. Gene expression patterns define key transcriptional events in cell-cycle regulation by cAMP and protein kinase A. Proc Natl Acad Sci USA. 2005;102(24):8561–8566. 10.1073/pnas.0503363102 [PubMed: 15939874]

56. van Oirschot BA, Stahl M, Lens SM, Medema RH. Protein kinase A regulates expression of p27(kip1) and cyclin D3 to suppress proliferation of leukemic T cell lines. J Biol Chem. 2001;276(36):33854–33860. 10.1074/jbc.M104395200 [PubMed: 11457838]

57. Lee SH, Reed-Newman T, Anant S, Ramasamy TS. Regulatory role of quiescence in the biological function of cancer stem cells. Stem Cell Rev Rep. 2020;16(6):1185–1207. 10.1007/s12015-020-10031-8 [PubMed: 32894403]

58. De Angelis ML, Francescangeli F, La Torre F, Zeuner A. Stem cell plasticity and dormancy in the development of cancer therapy resistance. Front Oncol. 2019;9:626. 10.3389/fonc.2019.00626 [PubMed: 31355143]

59. Brown JA, Yonekubo Y, Hanson N, et al. TGF-beta-induced quiescence mediates chemoresistance of tumor-propagating cells in squamous cell carcinoma. Cell Stem Cell. 2017;21(5):650–64 e8. 10.1016/j.stem.2017.10.001 [PubMed: 29100014]

60. Chen W, Dong J, Haiech J, Kilhoffer MC, Zeniou M. Cancer stem cell quiescence and plasticity as major challenges in cancer therapy. Stem Cells Int. 2016;2016:1740936. 10.1155/2016/1740936 [PubMed: 27418931]

61. Parish AJ, Nguyen V, Goodman AM, Murugesan K, Frampton GM, Kurzrock R. GNAS, GNAQ, and GNA11 alterations in patients with diverse cancers. Cancer. 2018;124(20):4080–4089. 10.1002/cncr.31724 [PubMed: 30204251]

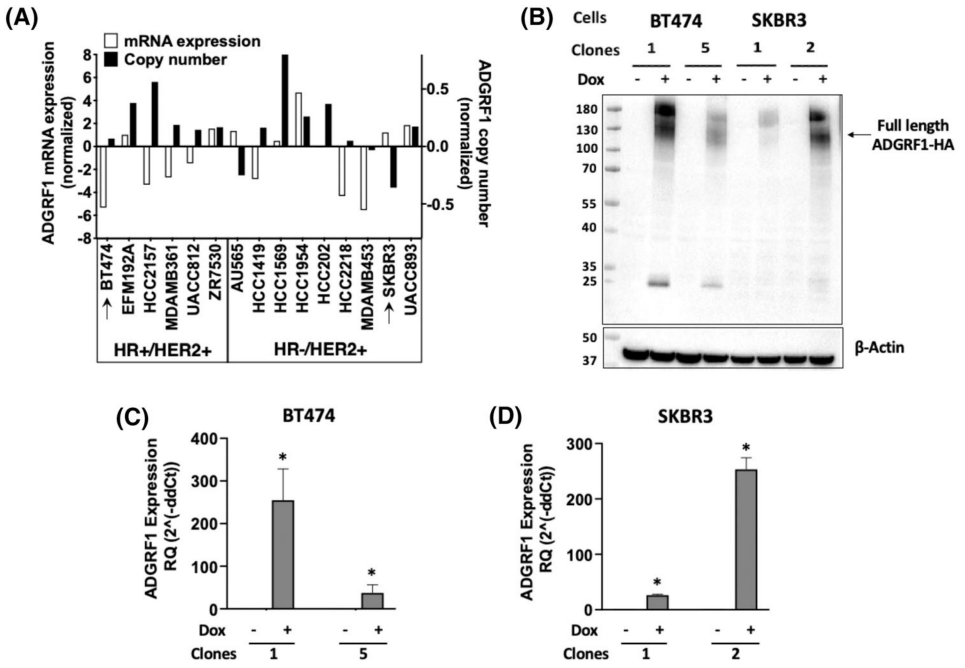

FIGURE 1.

ADGRF1 overexpression using pHAGE lentiviral-mediated infection of BT474 and SKBR3 parental cells. A, The normalized values of ADGRF1 mRNA expression and copy number in panel of HER2+ cell-lines from publicly available CCLE dataset. Arrows indicate two cell-lines with low ADGRF1 mRNA expression and copy number (BT474 and SKBR3), which were used to generate stable doxycycline (Dox)- inducible ADGRF1 overexpressing clones. B, immunoblotting analysis to detect the expression of full length ADGRF1 using anti-HA antibodies in clones 1 and 5 of BT474 cells and clones 1 and 2 of SKBR3 cells in absence (−) or presence (+) of Dox. Representative blot is shown from immunoblotting performed every 2 months during ongoing experiments. C and D, qRT-PCR showing the expression of full-length ADGRF1 in clones 1 and 5 of BT474 cells and clones 1 and 2 of SKBR3 cells grown in −/+ Dox. *indicates statistically significant difference compared to −Dox; $P < .05$ by unpaired t test (N = 5)

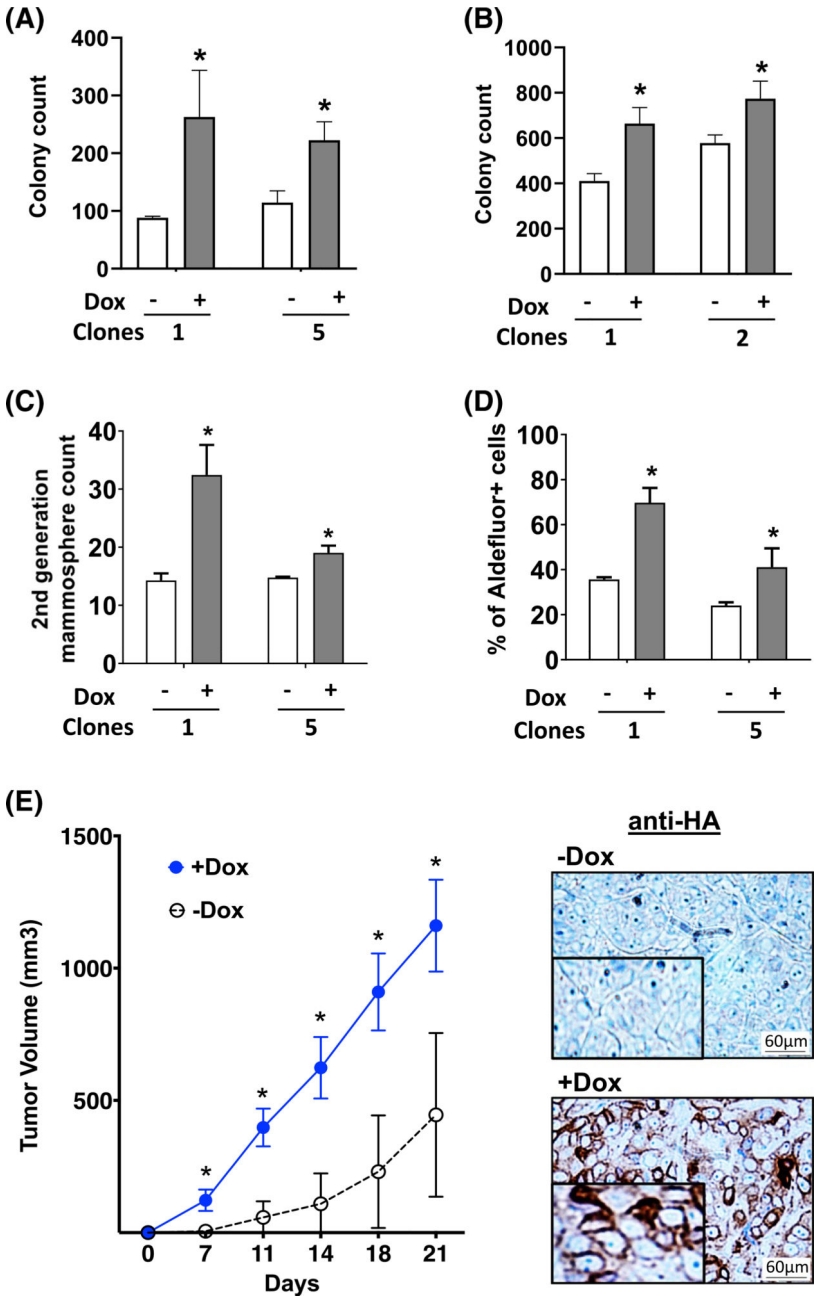

FIGURE 2.

ADGRF1 overexpression increased anchorage-independent cell growth, mammosphere formation, and Aldefluor positivity of HER2+ BC cells in vitro and increased the rate of tumor growth in vivo. BT474 clones 1 and 5 and SKBR3 clones 1 and 2 were grown in absence (−) or presence (+) of doxycycline (Dox). A,B, Anchorage-independent cell growth by soft agar assay. C, Mammosphere formation assay. D, Aldefluor assay using FACS analysis. E, For in vivo studies, 1 million BT474 clone 1 cells grown in +Dox or −Dox for 72 hours, confirmed for ADGRF1 overexpression in +Dox versus −Dox using anti-ADGRF1 antibody, were injected subcutaneously in athymic nu/nu mice (n = 10 per group). Tumor growth was measured twice weekly. The rate of tumor growth was significantly higher in

+Dox group versus −Dox group. *indicates statistically significant difference compared to −Dox; $P < .05$ by unpaired t test (N = 3–4)

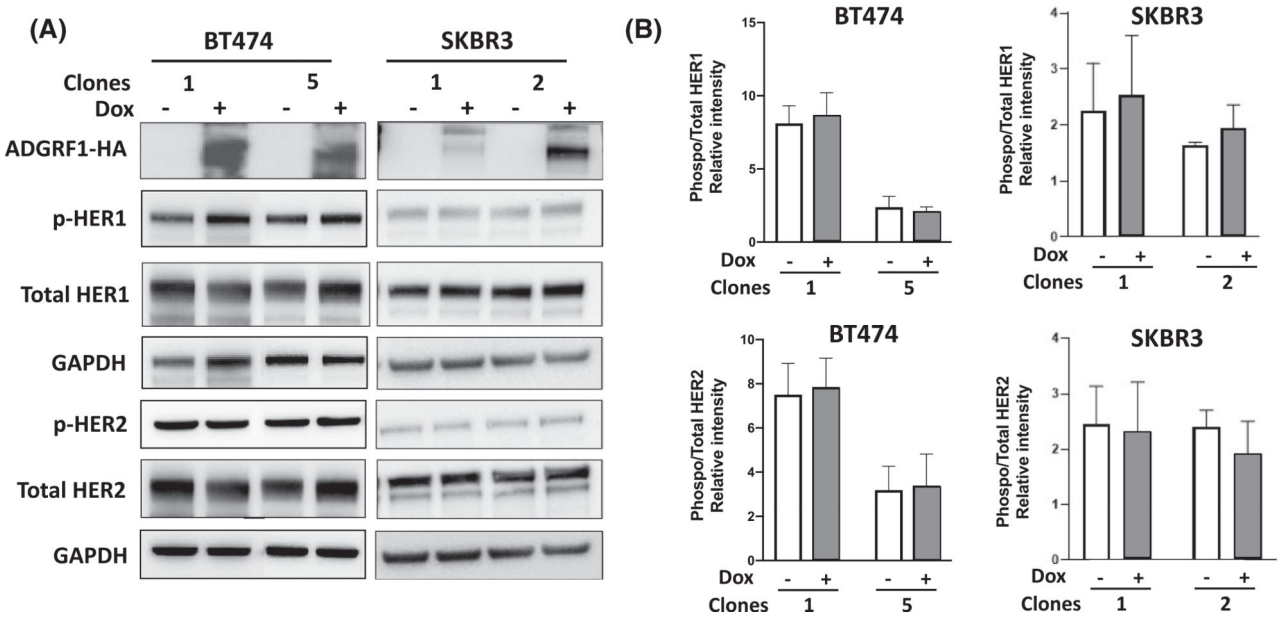

FIGURE 3.

ADGRF1 overexpression had no effects on total and phosphorylated HER1 and HER2 expression by immunoblotting. A, BT474 clones 1 and 5 and SKBR3 clones 1 and 2 were grown in absence (−) or presence (+) of doxycycline (Dox). After 72 hours of Dox treatment, protein was extracted, and the expression of phosphorylated HER1 and HER2 and total HER1 and HER2 was analyzed using immunoblotting. A representative immunoblot images of three individual replicates is shown. B, Densitometric quantitation of the relative intensity of phosphorylated (p)-HER1 and HER2 over total (t)-HER1 and HER 2 bands from three independent experiments (mean ± SEM). GAPDH was used as a loading control for visual assessment

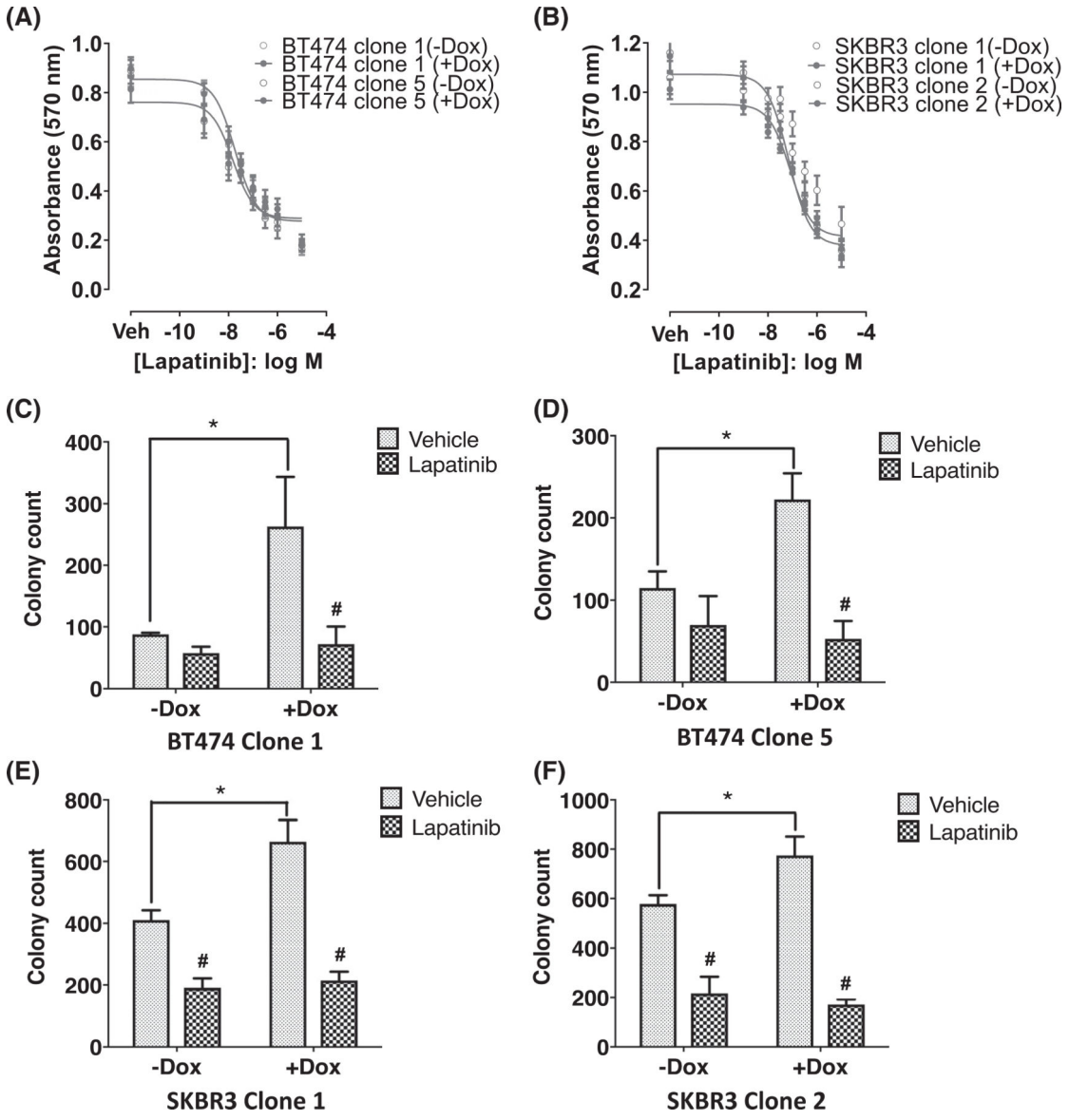

FIGURE 4.

ADGRF1 overexpression did not alter lapatinib activity on anchorage–dependent and –independent cell growth. BT474 clones 1 and 5 and SKBR3 clones 1 and 2 were grown in absence (−) or presence (+) of doxycycline (Dox) and in absence and presence of various concentrations of lapatinib for (A-B) the MTT assay or 1 nM of lapatinib for (C-F) soft agar assay (N = 3–4). For the determination of IC_{50} of lapatinib, and neratinib, the data was fitted using no-linear regression analysis and 3-parameter logistic equation: Y = Bottom + (Top-Bottom)/ (1 + 10^(*X*-LogIC50)) using GraphPad Prism version 8.0c. *indicates statistically significant difference compared to −Dox and indicates statistically significant difference compared to vehicle in the same Dox group by Two-way ANOVA; $P < .05$

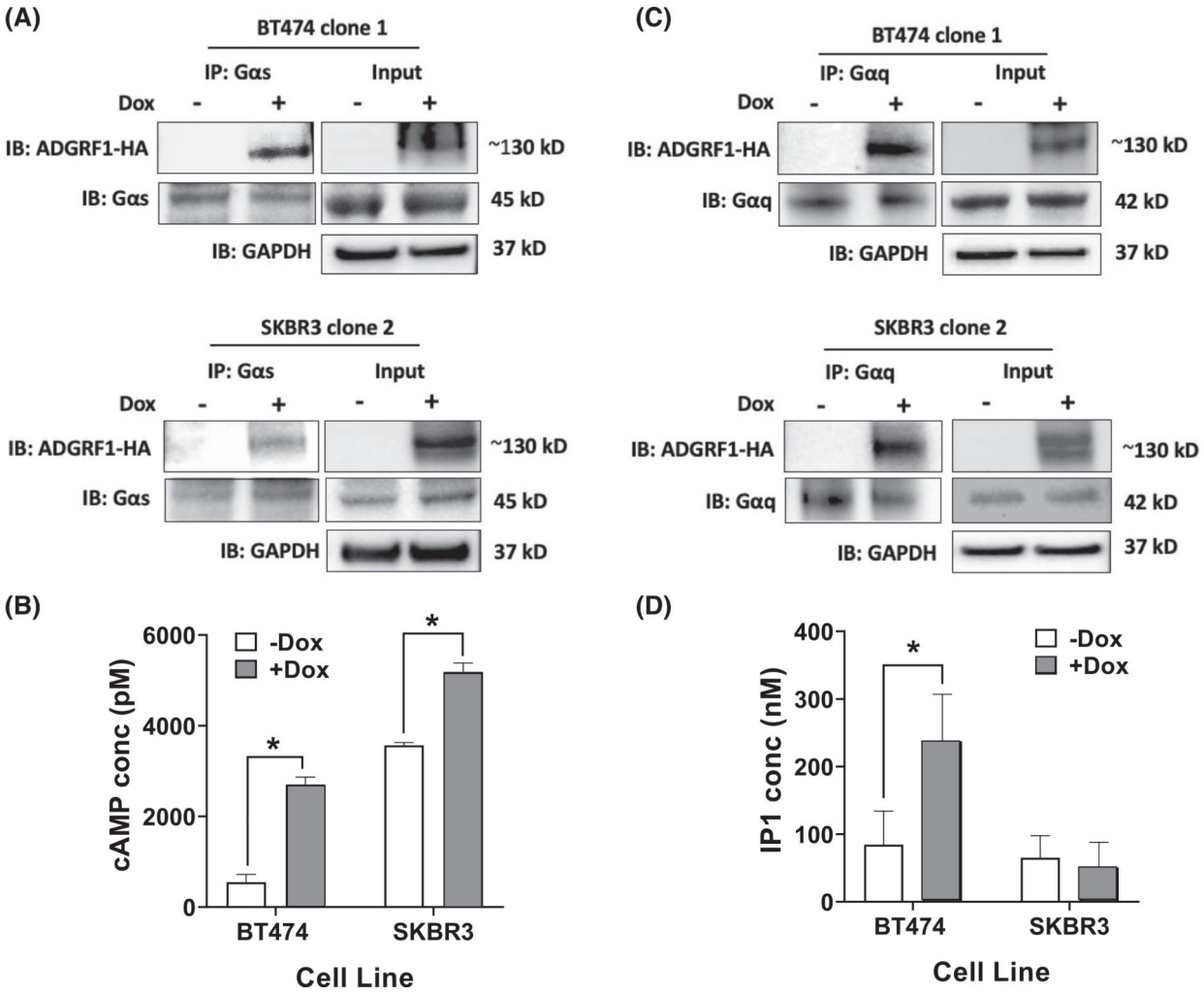

FIGURE 5.

ADGRF1 overexpression activates Gαs/Gαq pathways. BT474 clone 1 and SKBR3 clone 2 were grown in absence (−) or presence (+) of doxycycline (Dox). A, Co-immunoprecipitation with anti-Gαs and immunoblotting with anti-HA indicate that ADGRF1 couples to Gαs in both BT474 and SKBR3. B, Basal levels of cAMP were significantly increased upon ADGRF1 overexpression with Dox in both cells. C, Co–immunoprecipitation with anti-Gαq and immunoblotting with anti-HA indicate that ADGRF1 couples also to Gαq in both cells. D, Basal levels of IP1 were significantly increased upon ADGRF1 overexpression with Dox in BT474 but not SKBR3 cells. *indicates statistically significant difference $P < .05$ by unpaired t test (N = 3–4)

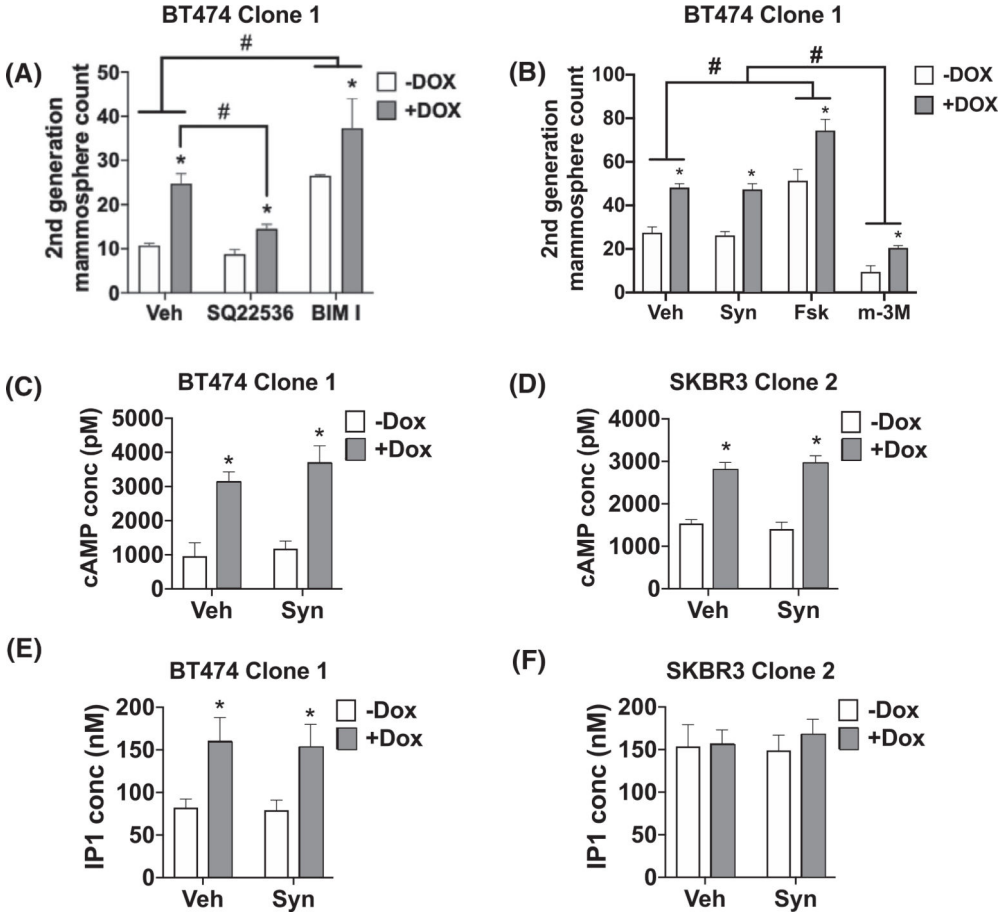

FIGURE 6.

ADGRF1 coupling to Gαs pathway is pro-tumorigenic. BT474 clone 1 and SKBR3 clone 2 were grown in absence (−) or presence (+) of doxycycline (Dox). A, Mammosphere formation assay showing that SQ22536 (100 μM) decreased secondary mammospheres compared to Vehicle (Veh) in +Dox cells only. Whereas BIM I (10 μM) increased the number of secondary mammospheres compared to vehicle (Veh) in both −Dox and +Dox cells, B, Mammosphere formation assay showing that Forskolin (Fsk, 10 μM) increased whereas m-3M3FBS (m3M, 50 μM) decreased the number of secondary mammospheres compared to vehicle (Veh) in both −Dox and +Dox cells. Synaptamide (Syn, 10 nM) showed no change in secondary mammospheres compared to Veh in both −Dox and +Dox cells. Synaptamide (Syn, 10 nM) did not alter basal levels of cAMP upon ADGRF1 overexpression in (C) BT474 Clone 1 or in (D) SKBR3 Clone 2. Synaptamide (Syn, 10 nM) did not alter basal levels of IP1 upon ADGRF1 overexpression in (E) BT474 Clone 1 or in (F) SKBR3 Clone 2. *indicates statistically significant difference compared to −Dox by unpaired *t* test, $P < .05$. #indicates statistically significant difference between various treatment groups; $P < .05$ by Two-way ANOVA, Sidak's multiple comparisons test, (N = 3–4)

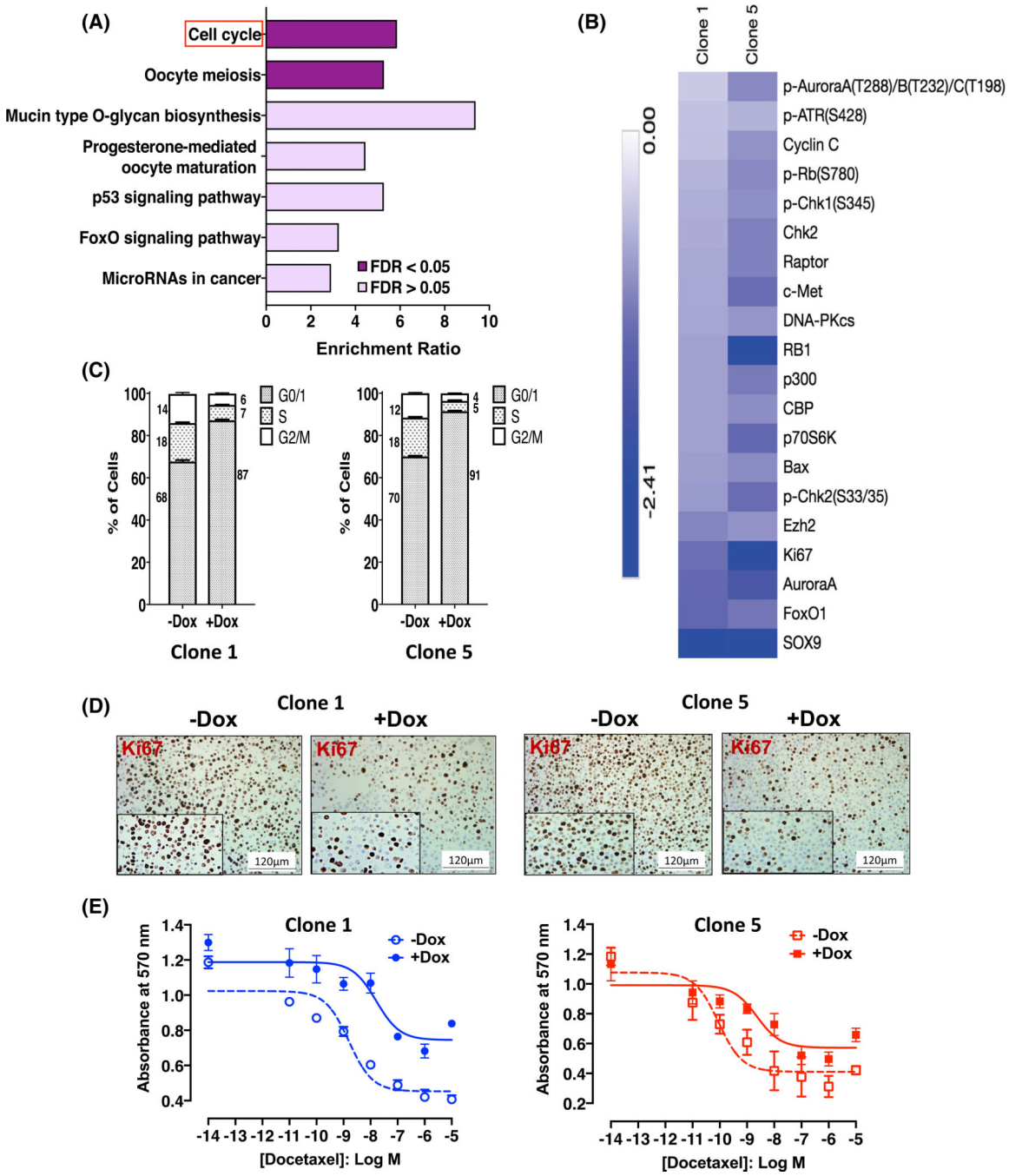

FIGURE 7.

Bioinformatic analysis and validation studies identify cell cycle arrest and chemoresistance indicating promotion of quiescence with ADGRF1 overexpression in HER2+ BC. BT474 clones 1 and 5 were grown in absence (−) or presence (+) of doxycycline (Dox) for 72 hours. A, RNAseq analysis was performed (N = 2, each in triplicates) and Over-Representation Analysis (ORA) using 663 differentially expressed downregulated genes with a false discovery rate (FDR) *q*-value < .05 showed eight enriched pathways with FDR *q*-value < .1 and two pathways with FDR *q*-value < .05, and the enrichment score was plotted as

enrichment ratio. B, RPPA analysis was performed (N = 3, each in triplicates) and the heatmap showing the common downregulated proteins related to cell cycle upon ADGRF1 overexpression with FDR q value < .05. C, Cell cycle analysis (N = 3) showing G0/1 arrest induced by ADGRF1 overexpression. D, A reduction in Ki67 expression upon ADGRF1 overexpression was confirmed using IHC in BT474 clones 1 and 5. E, MTT assay was performed for cells grown with various concentrations of docetaxel (N = 3). ADGRF1 overexpression led to about 10-fold reduction in docetaxel potency, suggesting chemoresistance

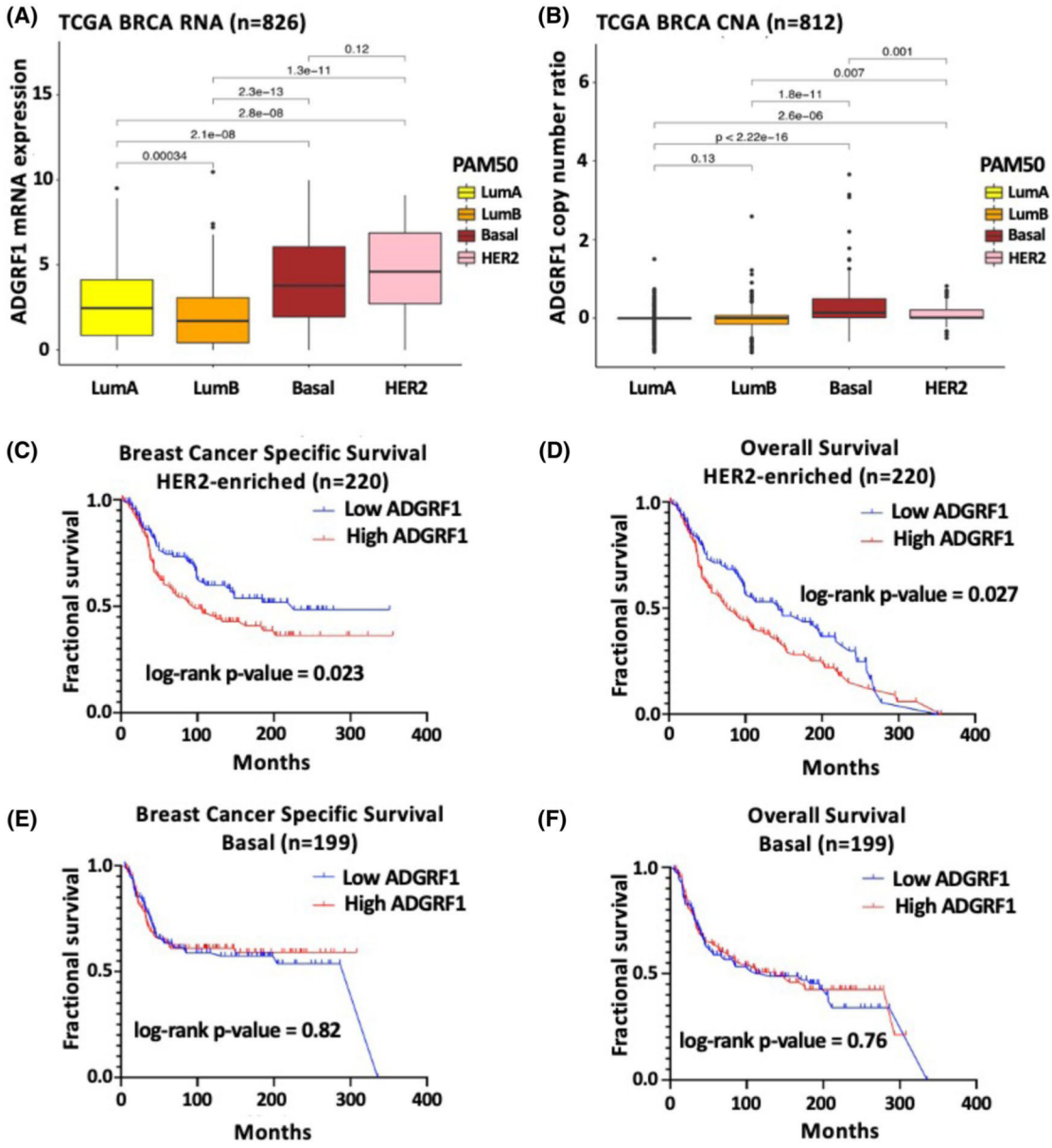

FIGURE 8.

ADGRF1 is overexpressed and amplified in HER2-enriched and basal subtypes of breast cancer and predict BCSS and OS in HER2-enriched but not basal subtypes. Analysis of The Cancer Genome Atlas (TCGA) RNA-Seq and copy number dataset (http://gdac.broadinstitute.org/) showing: A, *ADGRF1* RNA expression; and B, corresponding copy number alterations in different BC subtypes. At RNA level, *ADGRF1* gene expression was significantly higher in HER2+ and basal subtypes compared to luminal A and B BCs (Wilcoxon test, $P < .05$). *ADGRF1* gene was amplified in basal and HER2+ subtypes of BC (Wilcoxon test, $P < .05$). C-F, Survival curves using METABRIC database in patients with HER2-enriched and basal BC subtypes with high versus low *ADGRF1* expression. Kaplan-Meier curves for BC-Specific Survival (left panel) and Overall Survival (right panel) of

patients with; (C and D) HER2-enriched (n = 220); and (E and F) basal (n = 199) BC subtypes with high versus low expression of *ADGRF1*

TABLE 1

Lapatinib and neratinib IC_{50} values (reported as mean ± standard error of mean)

Drug	BT474 Clone 1	BT474 Clone 5	SKBR3 Clone 1	SKBR3 Clone 2
Lapatinib (nM)				
−Dox	20.4 ± 8.1	31.2 ± 22.2	141.9 ± 13.3	208.7 ± 55.6
+Dox	30.6 ± 18.5	13.9 ± 7.2	70.8 ± 12.1	125.4 ± 45.3
Neratinib (pM)				
−Dox	19.14 ± 1.78	31.51 ± 1.85	ND	ND
+Dox	19.29 ± 1.57	70.13 ± 1.50	ND	ND

ND, not determined.

TABLE 2

Docetaxel IC_{50} (in nM, reported as mean ± standard error of mean)

	BT474 Clone 1	BT474 Clone 5
−Dox	1.57 ± 1.1	0.089 ± 2.2
+Dox	16.27 ± 1.5	2.29 ± 1.2